Materials Today Sustainability 31 (2025) 101193

Contents lists available at ScienceDirect

Materials Today Sustainability

journal homepage: www.journals.elsevier.com/materials-today-sustainability

Green synthesis and characterization of titanium dioxide nanoparticles using Eucalyptus globulus leaf extract: Impacts of the mild thermal treatment

Abouelkacem Sahraoui [a,c], Mouna Hamlaoui [a], Sara Chikhi [a], Safia Harrat [b], Oualid Baghriche [a], Abdennour Zertal [a,*], Sergio Vernuccio [c,d]

[a] Laboratory of Innovative Environmental Preservation Techniques, Department of Chemistry, Constantine 1 Frères Mentouri University, Algeria
[b] Laboratory of Ceramics, Department of Physics, Constantine 1 Frères Mentouri University, Algeria
[c] Department of Chemical and Biological Engineering, University of Sheffield, UK
[d] School of Chemistry and Chemical Engineering, University of Southampton, UK

ARTICLE INFO

Keywords:
Green synthesis
Thermal treatment
Eucalyptus globulus leaf extract
Titanium dioxide nanoparticles
Characterisation

ABSTRACT

Current research efforts are directing considerable attention towards the green synthesis of nanomaterials, such as titanium dioxide nanoparticles (NPs) known for their versatile technological applications. The present work is the first to report on the synthesis of TiO_2 NPs using eucalyptus globulus leaf extract - a gentle, renewable, and non-toxic agent - in conjunction with titanium butoxide as a precursor in a mild thermal treatment. The results comprise four distinct biosynthesised material samples, each obtained by applying different techniques, including single and double-thermal treatments of NPs. Initially characterized by Fourier-transform infrared (FT-IR) and UV–visible spectroscopy, the plant extract plays a dual role in both reduction and stabilisation, leading to a remarkable NPs stability. The phytochemicals components, including phenolic and flavonoid acids, are believed to reduce the Ti^{4+} ions, aiding in the creation of related NPs. The successfully synthesised TiO_2 samples were characterised with diffuse reflectance UV–visible spectroscopy (DRS), FT-IR, Raman, X-ray powder diffraction (XRD), and scanning electron microscopy with energy dispersive X-ray spectroscopy (SEM-EDX). The findings from these investigations highlighted the pure, uniform structure, and arrangement of all NP samples, exhibiting a spherical morphology and a predominance of the anatase form. The characteristic parameters of the NPs including particle size, band gap energy, crystallinity, and lattice constants, were calculated and compared to those of commercial TiO_2. The double thermally treated sample exhibits a closer resemblance to commercial TiO_2 compared to both the singal thermally treated sample and the untreated counterpart. This suggests that the proposed mild thermal treatment can serve as an alternative approach for the effective and environmentally friendly preparation of TiO_2 NPs, ensuring good physico-chemical characteristics for a broad spectrum of advanced and sustainable applications.

1. Introduction

Over the past few decades, there has been a growing interest in nanotechnology research. Scientists across a wide range of disciplines and fields have shown interest in these advancements, envisioning their potential applications, particularly in the synthesis of metal oxides such as TiO_2 and ZnO [1,2]. The former is a well-known versatile semiconductor that is essential to many different catalytic and photocatalytic applications, including air treatment, water splitting and purification [3,4]. TiO_2 plays a key role in gas sensing [5], solar energy conversion [6], and development of nanostructured coatings for biomedical implants, due to its material properties and nanoscale chemical reactivity [7]. Additionally, it demonstrates efficacy in adsorbing larger amounts of dye molecules [8]. The good physical stability and non-toxicity of TiO_2 position it as one of the most researched nanoparticles (NPs) [9]; nevertheless, studying nanostructures requires a deeper comprehension

* Corresponding author. Department of Chemistry, Constantine 1 - Frères Mentouri University, Aïn El-Bey Street, 25000, Constantine, Algeria.
E-mail addresses: abouelkacem.sahraoui@doc.umc.edu.dz (A. Sahraoui), hamlaoui.mouna@umc.edu.dz (M. Hamlaoui), sara.chikhi@doc.umc.edu.dz (S. Chikhi), safia.harrat@student.umc.edu.dz (S. Harrat), oualid.baghriche@umc.edu.dz (O. Baghriche), abdennour.zertal@umc.edu.dz (A. Zertal), s.vernuccio@soton.ac.uk (S. Vernuccio).

https://doi.org/10.1016/j.mtsust.2025.101193
Received 8 April 2024; Received in revised form 21 July 2025; Accepted 5 August 2025
Available online 7 August 2025

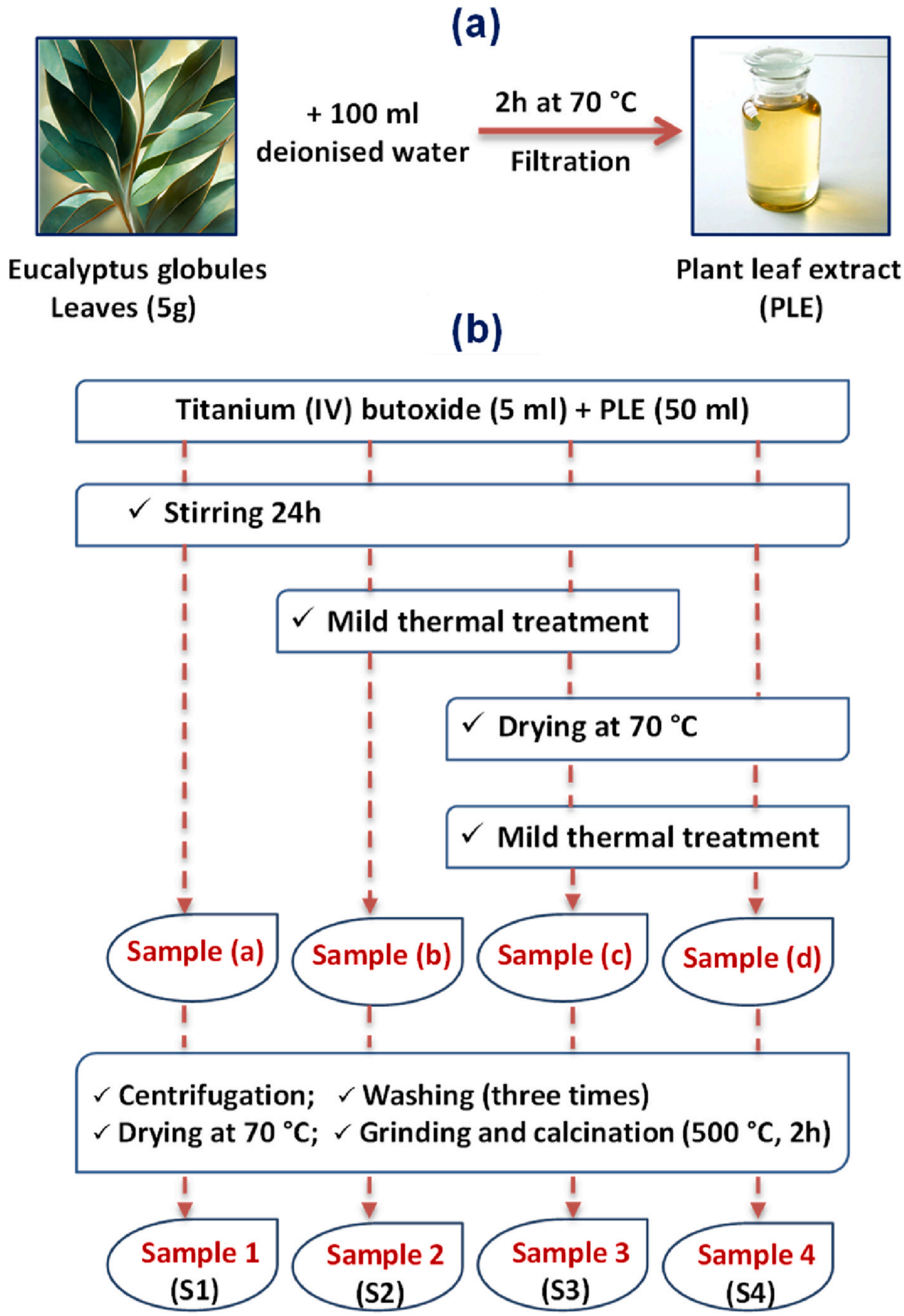

Fig. 1. Steps involved during TiO_2 NPs synthesis by Eucalyptus globules leaf extract: a) Preparation of the Plant Leaf Extract (PLE) b) Preparation of different TiO_2 NPs samples.

of the crystal form with flexible structures, which can be attained by novel, low-tech production techniques and designs [10]. Given this, there is a plethora of literature on TiO_2 synthesis, which produces nanoparticles of varying sizes, morphologies, and crystalline phases [11,12]. Several studies have extensively explored the advantages of wet chemistry, as a method for the synthesis of these nanocrystals. Among the reported techniques, sol-gel [13,14] and hydrothermal methods [15,16] stand out as recommended approaches. Sol-gel synthesis is the most straightforward, successful, affordable, and widely used technique for producing TiO_2 NPs with a range of morphologies, such as wires, aerogels, particles, rods, mesoporous, tubes, and sheets [1]. As an alternative, green preparation method, utilizing natural sources such as bacteria [17,18], plants [19,20], plant extracts [21,22], and other pure biodegradable materials [23,24] as preparation agents, have been recently proposed as novel synthesis approaches. These environmentally friendly techniques have shown significant advancements in the synthesis of NPs across various materials, owing to their low toxicity, stability, and cost effectiveness [21,25–27]. The adoption of these approaches has exerted a transformative impact on many scientific disciplines, including physics, chemistry, biology, and material sciences [28]. Moreover, plant extracts (flower, fruit, leaf, peel, root and stem as source) have been proposed as reagents in several recent articles on NPs synthesis, due to their perceived safety and applicability in industrial production [29]. Operational variables such as temperature, pH, and precursor concentration can have a significant influence on the morphology, size, shape, porosity, and crystallinity of the NPs [30,31]. However, the specific process by which phytochemicals induce the synthesis of NPs remains unclear.

The Myrtaceae family of flowering plants includes Eucalyptus globulus, which has long been used as a traditional medicinal plant to cure a variety of illnesses. This tall, evergreen tree is characterized by mostly smooth bark, juvenile leaves that are whitish and waxy on the lower surface, glossy green, lance-shaped adult leaves, glaucous, and ribbed flower buds [32]. Much information about using eucalyptus leaf extracts to prepare metallic [33–35] or bimetallic NPs [36] has been obtained and reported in recent years. Flavonoids, alkaloids, chlorophylls [37], alcoholic chemicals, ketones, and amines that function as reducing and capping agents are all present in eucalyptus leaf extracts [36]. Ethers, alcohols, amides, terpineols, aldehydes, and eucalyptols were also detected by GC-MS analysis, according to Jin et al. [38]. More recently, LCMS indicated the existence of 41 polyphenols as extract ingredients [39].

Given the abundance of Eucalyptus globulus in the north of Algeria and the hypothesis that phytochemicals are crucial to the NPs synthesis, Eucalyptus leaf extract was utilised in this investigation as a precursor for the synthesis of TiO_2 NPs. For the first time, the impact of the synthesis process, involving stirring the TiO_2 suspension at 90 °C for 24 h, on the optical, structural, and morphological properties of the biosynthesised TiO_2 NPs was examined using various characterization techniques, including Diffuse Reflectance Spectroscopy (DRS), X-ray diffraction (XRD), Fourier transformed infrared (FT-IR), scanning electron microscopy with energy dispersive X-ray (SEM-EDX), and Raman analysis. The physicochemical characterizations of commercial P25 and synthesised TiO_2 NPs were also compared.

2. Experimental

2.1. Chemicals

The present investigation used Eucalyptus globulus leaves as a bioreducing agent (Fig. 1). Thus, fresh leaves of Eucalyptus globulus were collected from the east region of Constantine (latitude of 36° 17′ N, longitude of 6° 37′ E), Algeria. Titanium (IV) butoxide (TB) (purity ≥97.0 %) was purchased from SIGMA-ALDRICH, and Commercial TiO_2 (Degussa P25) from INTERCHIM. All chemicals were used as received. Deionized water was used throughout the experiments for all syntheses.

2.2. Methods

TiO_2 NPs were synthesised in two stages (Fig. 1).

i) Preparation of the globular eucalyptus leaf extract: a simple, practical, and commonly used solid-liquid drying procedure was applied [10,22,40,41]. Fresh leaves were thoroughly washed with water to remove dust and dried at ambient room temperature before being sliced. 5 g of chopped, cleaned leaves were boiled with 100 mL of distilled water in a 250 mL Erlenmeyer flask for 2 h at 70 °C. After cooling and filtering through a 0.45 μm PTFE filter to remove particle debris, the transparent extract with a pleasant scent was stored in the fridge at 4 °C until use.
ii) Reaction with TB: the eco-friendly synthesis used in this study is a modified version of the method reported by Al Qarni et al. [41]. Additionally, for the first time, a mild thermal treatment was introduced in order to reduce the size of TiO_2 NPs. Four different methods (1–4) were analysed, resulting in four distinct biosynthesised material samples:

(1) In an Erlenmeyer flask, 5 mL of TB was added dropwise to 50 mL of the leaf extract while continuously stirring. The mixture was then stirred at room temperature overnight (sample a).
(2) Under a magnetic stirrer, 5 mL of TB was introduced dropwise to 50 mL of leaf extract in a Pyrex reactor equipped with a double envelope allowing water circulation and linked to a circulator bath (room temperature). The resulting heterogenious solution was covered and stirred overnight at 90 °C (sample b). In this work, we refer to this stage as the mild thermal treatment.
(3) The third process is similar to the second, except that TiO_2 was collected and dried at 70 °C before being added to 50 mL of ultrapure water in the Pyrex reactor. The resulting solution was covered and stirred overnight to undergo the same thermal treatment at 90 °C (sample c).
(4) The fourth method combines the first and second phases of processes (1) and (3). Thus, in an Erlenmeyer flask, 5 mL of TB was added dropwise to 50 mL of the leaf extract and stirred overnight at room temperature. The TiO_2 suspension was collected and dried at 70 °C before being added to 50 mL of ultrapure water in the Pyrex reactor to undergo the same thermal treatment (sample d).

The four samples (a, b, c, and d) were centrifuged at 10^4 rpm for 15 min and washed three times before drying in an oven at 70 °C. The dry gels were ground and calcined for 2 h at 500 °C to produce four bright white TiO_2 nanoparticle powder samples (designated as S_1, S_2, S_3, and S_4, respectively), which were then stored in sealed glass containers ($m_{sample} \approx 1$ g).

2.3. Characterization

2.3.1. UV–vis analysis

The globular eucalyptus leaf extract light absorption spectrum was obtained at room temperature using UV–Vis spectrometry (UV1800, Shimadzu Corp. Tokyo, Japan), while diffuse reflectance UV–vis spectroscopy was performed on a Jasco V-750 spectrophotometer (Japan) outfitted with an ISV-922 integrating sphere and VWSP-966 SPF/PA calculation program. The TiO_2 samples were analysed in their solid powdered form. The reflectance data were then converted to absorbance using the Kubelka-Munk function. This analysis aimed to obtain and assess the optical characteristics and structures of TiO_2 NPs. All nanomaterials' spectra were obtained between 200 nm and 900 nm with a 1 nm resolution at ambient pressure and temperature. This aided in illustrating the electronic absorption spectrum.

2.3.2. XRD analysis

To identify the crystal phase and estimate the crystallite size using Scherrer equation, the commercial and synthesised TiO_2 NPs were examined by X-ray Diffraction using a Shimadzu LabX XRD-6100 diffractometer set to 40 kV and 30 mA, with Ni filtered Cu Kα (l = 1.5406 Å) radiation with a scan speed of 2°/min from 20° to 80° (scan range) and diffraction angles of 2θ.

2.3.3. FT-IR and Raman analysis

Fourier Transform Infrared (FT-IR) and Raman spectroscopy analysis were conducted to confirm the NPs structure, using the Shimadzu Affinity 1-S (FT-IR) spectrometer and the Jasco RFT-6000 Raman spectrometer, respectively. The samples were shaped into pellets with KBr for the infrared absorption spectra and the analyses were carried out in the transmittance mode in the 400–4000 cm^{-1} frequency range. The Raman spectra were recorded directly on the pure powdered samples without any additional chemical preparation using a 532 nm laser. The spectral range was recorded from 100 to 1000 cm^{-1} with a spectral resolution of approximately 2 cm^{-1}. Both techniques confirmed the characteristic vibrational modes of TiO_2, with Raman spectroscopy providing additional phase identification through lattice vibrations.

2.3.4. SEM and EDX analysis

The microstructural and elemental analyses of the samples were performed using a field emission scanning electron microscope (FE-SEM) ZEISS Gemini 450, coupled with a Bruker X-Flash 6460 Energy Dispersive X-ray (EDX) detector. SEM imaging was used to investigate the surface morphology, particle size, and phase distribution of the

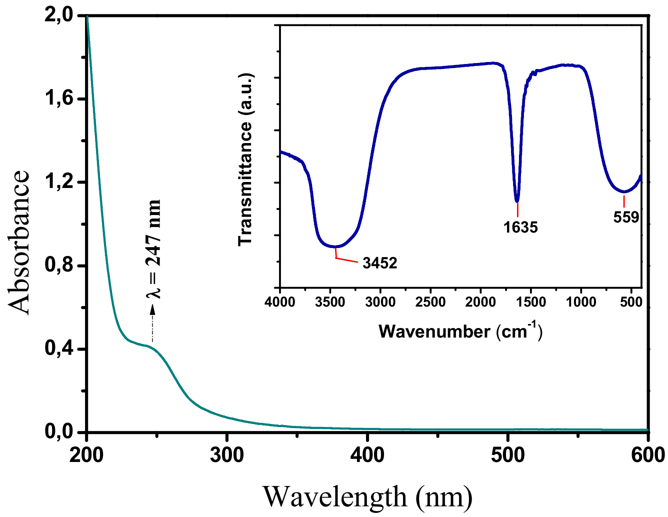

Fig. 2. Eucalyptus globules leaf extract characterisation: UV–Vis spectrum, inset: FTIR spectra.

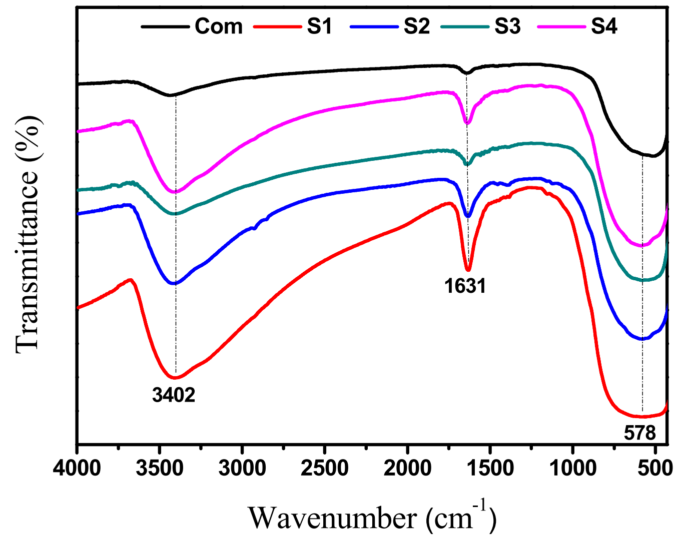

Fig. 4. FTIR spectrum of commercial (com) and green synthesised TiO_2 NPs.

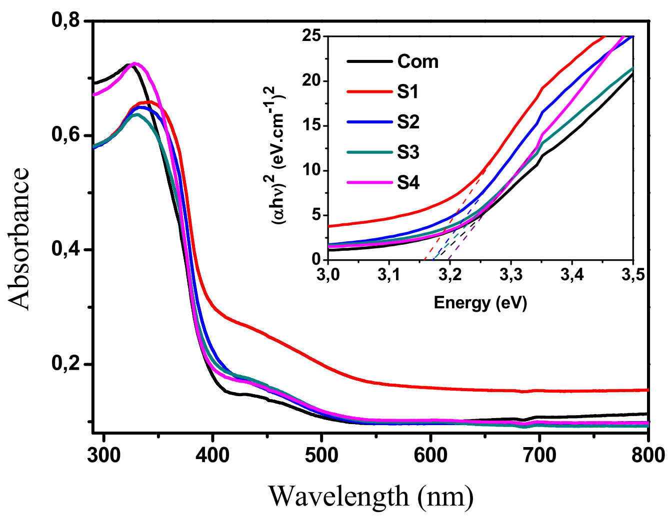

Fig. 3. UV–Visible diffuse reflectance spectra of commercial (com) and synthesised TiO_2 NPs. Inset: UV–Vis spectra Tauc plot.

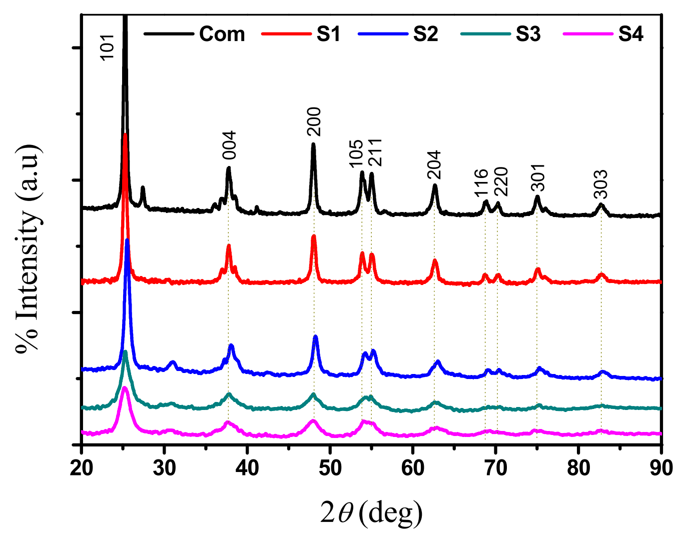

Fig. 5. XRD patterns of the commercial (com) and synthesised TiO_2 NPs.

samples. The powdered samples were mounted on aluminium stubs using carbon adhesive tape and sputter-coated with a thin layer of gold (approx. 5 nm) to enhance conductivity. SEM images were captured under high-vacuum mode at an accelerating voltage of 15 kV, with a working distance of approximately 8–10 mm, and magnifications ranging from 1000 × to 20,000 × . EDX analysis was conducted on selected areas to determine the elemental composition and distribution. Spectra were acquired at the same accelerating voltage, with an acquisition time of 60 s per area. This combined SEM/EDX technique provided comprehensive information on both the structural and chemical characteristics of the materials.

3. Results

3.1. Characterization of eucalyptus leaf extract

The physicochemical properties of Eucalyptus leaf extract can assist in explaining the mechanism of TiO_2 NPs formation. Furthermore, the nature of the produced nanostructured materials can have a significant impact on their performance in several fields. The UV–vis spectrum of the Eucalyptus globulus extract solution (Fig. 2) shows only a broad shoulder around 147 nm, which can be assigned to the $\pi \rightarrow \pi^*$ transition of aromatic C=C bonds. This result, which is consistent with previous findings, could be attributable to the main phytochemical components of the bio-reducing agent, such as phenolics, tannins, and flavonoids [38,42].

The functional groups present in the plant extract are well known to play a significant role in the TiO_2 reduction into NPs. Therefore, to confirm their existence and identify those involved in the conversion reaction, the Fourier transform infrared spectra of the plant extract is frequently examined. Fig. 2 (insertion) depicts the FTIR spectra of Eucalyptus globulus leaf extract. The O-H group's stretching vibration is shown by the broad absorption peak at 3452 cm^{-1}. The aromatic ring is represented by the absorption peak at 1635 cm^{-1}, and the aromatic C-H group by the second broad absorption pattern at 559 cm^{-1}. These peaks are related to typical mono-, di-, and tri-substituted benzene rings, from eucalyptols, terpineols, alcohols, amides and ethers and other essential oil components. Overall, the interpretation of FTIR spectra from our study is well supported by previous investigations [38,43].

Table 1
Powder XRD and SEM characterization analysis of synthesised and commercial (com) TiO_2 NPs.

Com TiO_2	*2θ*				*hkl values*	*Structure*		*Cells parameters (A°)*	*Average[a] crystallites size (nm)*	*Size[b] range (nm)*
	S1	S2	S3	S4						
25.27	25.30	25.32	25.27	25.27	(101)	anatase	***ComTiO₂***	a = 3.7892 c = 9.5370	12–17	10–13
37.69	37.80	37.84	37.69	37.68	(004)	anatase	***S1***	a = 3.7848 c = 9.5124	20–24	18–23
47.99	48.03	48.07	47.98	47.98	(200)	anatase	***S2***	a = 3.7822 c = 9.5023	18–22	17–21
53.76	53.89	53.93	53.76	53.76	(105)	rutile	***S3***	a = 3.7892 c = 9.5370	15–18	13–15
55.06	55.11	55.40	55.23	55.23	(211)	anatase	***S4***	a = 3.7892 c = 9.5370	19–23	18–22
62.57	62.69	62.75	62.75	62.57	(204)	rutile				
68.59	68.76	68.84	68.59	68.59	(116)	rutile				
70.48	70.67	70,67	70.42	70.15	(220)	anatase				
75.93	76.03	76.10	75.93	75.93	(301)	rutile				
82.63	82.80	83.14	82.80	82.63	(303)	anatase				

[a] XRD analysis.
[b] SEM analysis.

Table 2
Component ratio (EDX analysis) of synthesised and commercial TiO_2 NPs surface.

		Commercial	*S1*	*S2*	*S3*	*S4*
Weight (%)	Oxygen	20.01 *(40.36)*	21.87 *(40.56)*	27.12 *(42.58)*	19.78 *(38.11)*	24.85 *(43.60)*
(Atomic) (%)	Titanium	77.13 *(51.97)*	72.18 *(44.74)*	60.64 *(31.82)*	74.89 *(48.21)*	68.10 *(39.93)*
	Carbon	2.86 *(7.67)*	5.95 *(14.70)*	12.24 *(25.60)*	5.33 *(13.68)*	7.05 *(16.47)*

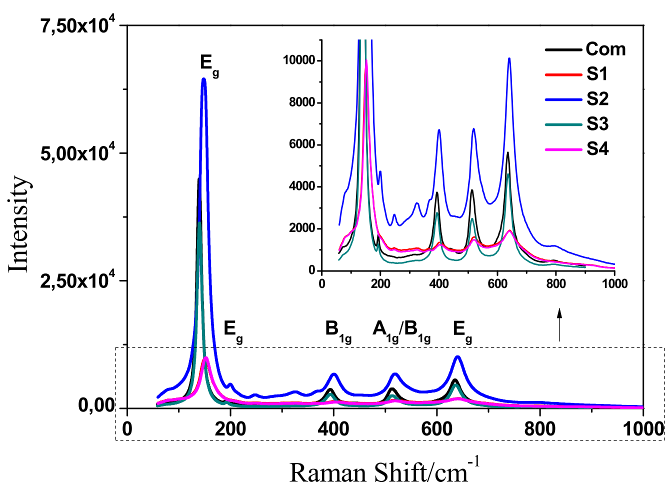

Fig. 6. Raman spectra of commercial (com) and synthesised TiO_2 NPs.

3.2. Characterization of synthesised TiO_2 nanoparticles

3.2.1. Optical properties

UV–vis spectroscopy is often used to ascertain the formation of metallic oxide nanoparticle by examining their optical characteristics [44]. Fig. 3 shows the UV–Vis diffuse reflectance spectra of commercial and synthesised TiO_2 NPs between 200 and 800 nm at room temperature. Overall absorbance versus wavelength patterns is consistent across all samples. As anticipated, the acquired spectra exhibit high UV absorption below 400 nm with distinct absorption maxima (λ_{max}), while the majority of light in the visible spectrum is reflected [45]. Sample S1, however, displays significant absorption in the visible light region. The emergence of TiO_2 NPs in the four synthesised samples was further supported by these findings. Unlike samples S1, S2, and S3, which exhibit maximum absorption bands at 339 nm, 334 nm, and 331 nm, respectively, sample S4 displays a maximum at 328 nm, which is well aligned with that of pure TiO_2 (325 nm).

The UV–visible spectrum of nanomaterials is generally used to evaluate the optical properties namely bandgap energy absorption edge (Eg). For this purpose, Equation (1) is typically adopted to calculate Eg using the Tauc plot, $(\alpha h\nu)^2$ *vs* $A(h\nu - Eg)$, which is derived assuming a direct transition between the edge of the valence band and conduction [22]:

$$(\alpha h\nu)^2 = A(h\nu - Eg) \quad (1)$$

where A is a constant, α is the optical-absorption parameter, and hν is the energy of a photon. E_g can be estimated by extrapolating the rectilinear portion of $(\alpha h\nu)^2$ *vs* hν to the x-axis. According to this equation, and as depicted in the inset of Fig. 4, the bandgap of the four samples (S1 to S4) falls within the range 3.16–3.20 eV. Notably, the band gap value of commercial TiO_2, was observed to be 3.18 eV, aligning well with the literature value of 3.22 eV. As a result, the biosynthesised TiO_2 nanopowders are deemed suitable for the nanooptic and electrooptical equipment fabrication.

3.2.2. FT-IR analysis

FTIR spectroscopy is generally used to investigate the potential interactions of NPs with various functional groups. This also implies that, during the bioreduction process, TB and the components of Eucalyptus globule leaf extract interact to form TiO_2 NPs [44,46]. Previous studies, which presented the synthesis of TiO_2 NPs using various techniques [44,47,48] support the overall interpretation of the FTIR spectra obtained in the present investigation.

As depicted in Fig. 4, the spectra of commercial TiO_2 and synthesised TiO_2 NPs exhibit remarkable similarity. However, the curves obtained for S3 and S4 are significantly closer to that of commercial TiO_2 than the other two samples (S1 and S2), indicating that the mild thermal treatment improves the quality, especially the purity, of the synthesised NPs. The FTIR spectrum shows three strong, separate peaks attributed to oxygen functional groups. The peak at 578 cm^{-1} corresponds to the stretching band of metallic oxygen (O-Ti-O) in the anatase morphology. Additionally, characteristic bands related to surface-adsorbed water (δ-H_2O) and hydroxyl groups are observed at 1631 cm^{-1} and 3402 cm^{-1} [22,41,44,49,50]. Furthermore, the absence of additional bands suggests that all organic compounds were successfully eliminated from the samples following calcination at 500 °C, underscoring the high purity of the NPs [49]. However, slight variations in peak intensities between the synthesised and commercial TiO_2 were observed, specifically, the intensity of the O-Ti-O stretching band (578 cm^{-1}). Several factors may contribute to this variation, including intrinsic material properties and

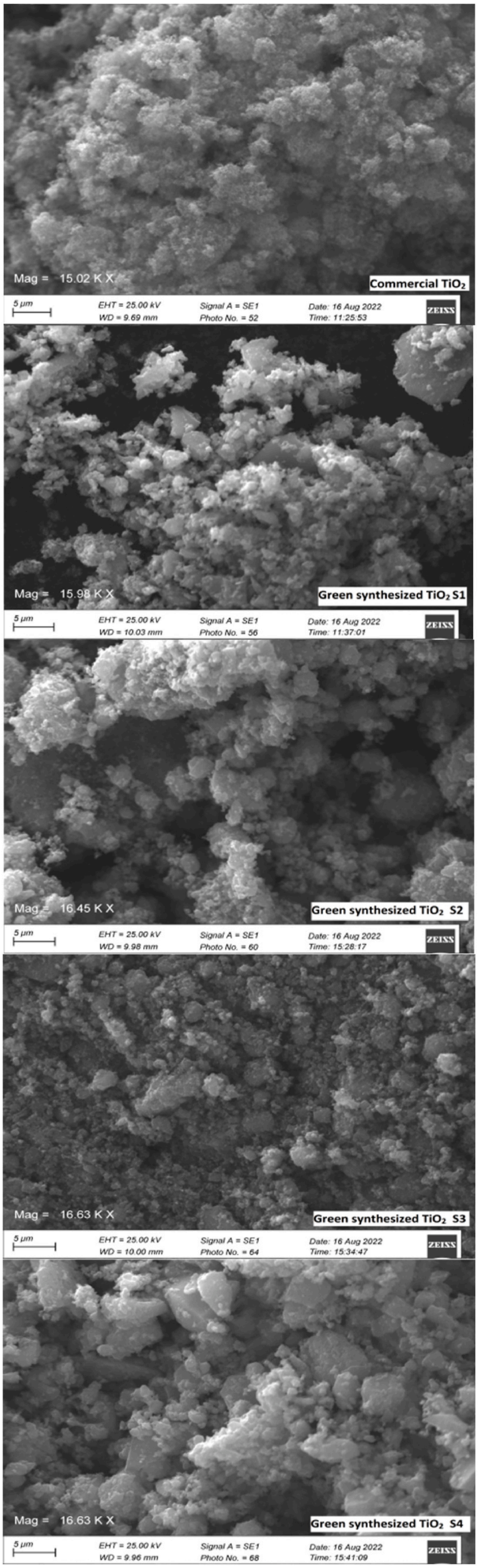

Fig. 7. SEM spectrum of commercial (com) and synthesised TiO_2 NPs.

potential experimental inconsistencies. In this study, the X-ray diffraction (XRD) spectra were overlaid in a single figure using OriginPro software, which may have led to an apparent narrowing of the peaks corresponding to the commercial TiO_2 sample. Nonetheless, such differences may also reflect slight variations in crystallinity, particle size, surface area, or phase composition between the samples [44,49,50].

3.2.3. XRD analysis

X-ray Diffraction (XRD) was employed to examine the average crystalline size, purity, crystalline phase, and crystalline structure of the commercial and synthesised TiO_2 NPs samples [31]. Fig. 5 displays the acquired XRD patterns, where the four synthesised samples exhibit the same peaks, 2θ values, obtained for commercial TiO_2. This confirms the successful formation of TiO_2 NPs derived from Eucalyptus globulus leaf extract and verifies their pure crystalline structure, as evidenced by the absence of any impurity peaks. Table 2 provides a summary of all recorded outcomes, including ten diffraction peaks corresponding to the planes of the tetragonal body-centred titanium dioxide (101, 004, 200, 105, 211, 204, 116, 220, 301, 303, and 204) (JCPDS N^{o}. 01-071-1167 and 01-084-1286). Compared to other peaks, the (101) orientation exhibits higher intensity, indicating its predominant presence. This JCPDS number was also utilised to verify that the patterns observed at 25.5, 38.5, 48.2, and 55.4° matched the anatase structure of the NPs, whereas the rutile structure was represented by those at 54.0, 62.0, 69.0, and 76.5° [19,20,51]. In this regard, it is worth noting that, according to supplier data, commercial TiO_2 typically comprises approximately 80 % anatase and 20 % rutile. However, the predominant presence of anatase in the four samples (S1, S2, S4, and S4) can be attributed to the presence of excess oxygen gas during the synthesis process, which slows down the rearrangement of Ti and O atoms and the subsequent conversion of anatase into rutile [23]. Moreover, the diffraction peak intensities decrease and broaden for the fourth sample suggesting a reduction in particle size [22,45].

Besides, the average crystalline size of TiO_2 nanoparticles was estimated using Sherrer's equation as follow:

$$D = \frac{K.\lambda}{\beta.\cos\theta} \tag{2}$$

where K is Scherer's constant (K = 0.94), λ is X-ray wavelength (0.1546 nm), β is the full width at half-maximum of diffraction line in radians (FWHM), θ is half diffraction angle, and *D* represents the average crystallite size. The obtained values in terms of average crystallite size and size range are reported in Table 1. Samples S3 and S4, which were subjected to the thermal treatment, exhibit smaller crystal sizes, measuring between 15 to 18 nm and 19–23 nm, respectively.

3.2.4. Raman analysis

The prevalence of the anatase phase in the NPs derived from the Eucalyptus globulus leaf extract was confirmed by Raman spectroscopy through the identification of the characteristic peaks associated with anatase. The Raman spectra of the synthesised NPs are displayed in Fig. 6, revealing a consistent pattern across all samples. Five different bands were observed for all the examined samples at 139, 197, 391, 513 and 634 cm^{-1}, aligning with the six Raman active phonon modes of TiO_2 anatase phase. These bands are respectively assigned to 3 E_g, 2 B_{1g}, and A_{1g}: 139 cm^{-1} (E_g), 197 cm^{-1} (E_g), 391 cm^{-1} (B_{1g}), 513 cm^{-1} (A_{1g} + B_{1g}), and 634 cm^{-1} (E_g) [41,52,53]. This result is reasonably consistent with the XRD findings and the Raman spectra. While the S3 bands closely overlay with the commercial TiO_2 counterparts, a slight frequency shift to higher values is observed in samples S1, S2, and S4. Additionally, the Raman bands of S4 exhibit a tendency to shift towards higher Raman intensity, particularly at 139 cm^{-1}. These shifts are commonly attributed to variation in structure, particle size, defect type, and other factors [53,54].

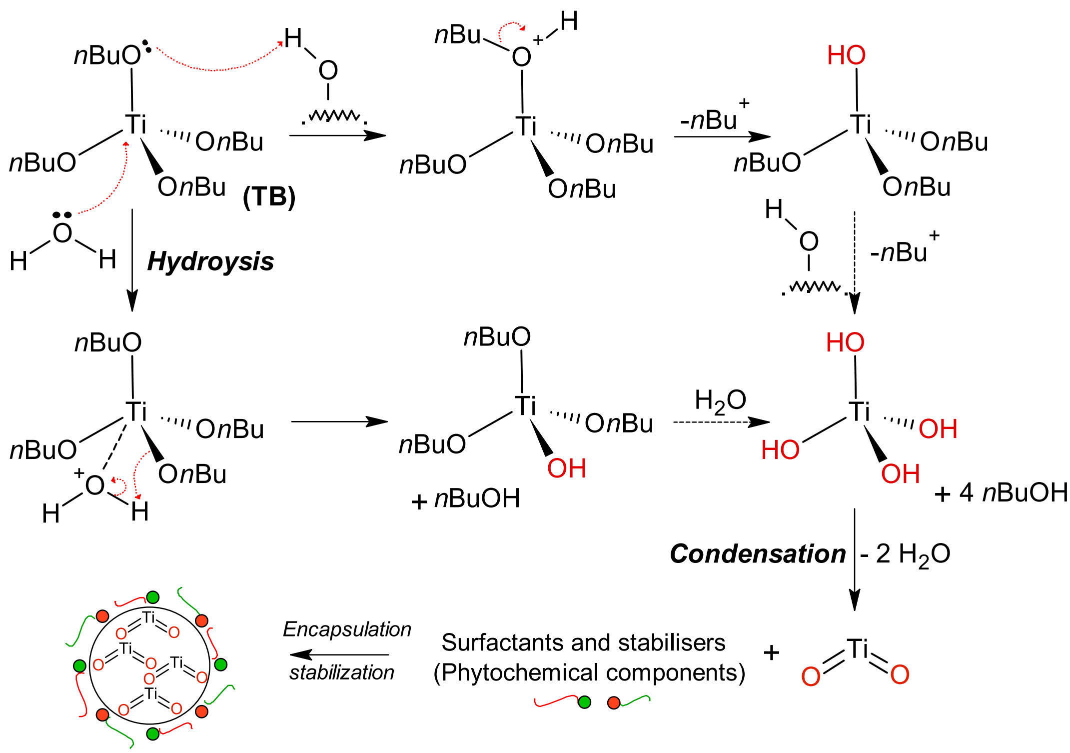

Fig. 8. Proposed mechanism of TiO_2 NPs synthesis by Eucalyptus globules leaf extract.

3.2.5. SEM-EDX analysis

Scanning Electron Microscopy (SEM) was used to investigate the morphology and the shape of both commercial and green-synthesised TiO_2 NPs (Fig. 7). The results of this analysis confirmed that the NPs agglomeration formed irregular structures, including quasi-spherical clusters. Table 1 summarises the calculated size range of the samples, which was plotted using the Image J programme. It is worth noting that the size (13–15 nm) closely resembles that of commercial TiO_2 (10–13 nm). Larger deviations were observed for the other synthesised samples.

The elemental composition of TiO_2 NPs samples was determined using SEM and EDX analysis. While peaks for Ti and O were clearly identified, a minor carbon peak emerged indicating the presence of an impurity derived from the Eucalyptus globulus plant extract. Table 2 provides the atomic compositions determined by EDX for each element. The surface of each sample exhibits a thick layer of titanium oxide growth. The synthesis of TiO_2 NPs, resulting from the hydrolysis of TB in a solution of ethanol or plant extract and water, has been shown to follow a similar pattern [55]. Additionally, titanium and oxygen are visible at remarkably similar concentrations in both commercial and S3 samples, with values of 51.97 %–40.36 % and 48.21 %–38.11 %, respectively. This underscores the similarity between sample S3 and commercial TiO_2. The observed behaviour is undoubtedly attributed to the utilization of a double thermal treatment during the S3 synthesis.

Based on the aforementioned results, we conclude that the structures of the synthesised NPs closely resemble those of commercial TiO_2. Therefore, it can be inferred that using the aqueous extract of Eucalyptus globulus leaf as a capping and stabilizing agent for the synthesis of nanostructured anatase is an effective approach for the improvement of the TiO_2 synthesis process towards sustainability. Moreover, the proposed mild thermal treatment appears to play a key role in the decomposition of dried precursors into nanocrystalline products.

4. Discussion

As previously noted, it is widely acknowledged that metal precursors can be reduced to metal oxide nanoparticles by plant extracts, which contain phytochemicals such as phenolic compounds, aldehydes, carbohydrates, flavonoids, terpenoids, and alkaloids [46,56].

In this study, Eucalyptus leaf extract, which incorporates several phytochemicals, *i.e.* eucalyptols, aldehydes, terpineols, alcohols, amides and ethers was used as the source for synthesizing TiO_2 NPs [38]. The FTIR study suggests that strong reducing agents, namely the hydroxyl and carbonyl groups in the plant extract, may be responsible for the bioreduction of titanium metal, which in turn leads to the formation of TiO_2 NPs. The sol-gel synthesis involved inorganic polymerization processes that occurred in solution using TB as a molecular precursor. Comprising four titanium-oxygen bonds, the TB molecule possesses two free electronic doublets on each oxygen atom, endowing it with nucleophilic, basic Lewis, and Brønsted properties which are essential for the reactivity of the precursor in the synthesis process. Due to its polarisation, the Ti-O bond is prone to ionic rupture, indicating the potential occurrence of nucleophilic attacks on the metal. Similar to other metallic alcoxides, TB easily undergoes reactions with water (i.e. hydrolysis). Additionally, it reacts with the phytochemicals extracted from Eucalyptus globulus leaves initiating the formation of hydroxides, as illustrated in Fig. 8. Following the formation of the hydroxyl groups, the condensation reaction takes place. This mechanism is in good agreement with various studies suggesting that the metal ions stabilize after being reduced by plant extracts by forming an organic coating in three distinct phases: (1) the complexing of Ti^{4+} with the aforementioned phytochemical in the mixed solution of Ti^{4+} and eucalyptus leaf extract; (2) the simultaneously reduction of Ti^{4+} by phytochemicals leading to the creation of TiO_2 NPs, and (3) encapsulation with alkanes, flavones, amines, and alcoholic chemicals [42,44,46].

While previous studies have explored the synthesis of TiO_2 NPs from various plant extracts, as well as the influence of several operating parameters such as pH, temperature, and contact time, the present study represents the first report, to our knowledge, investigating the effects of a mild thermal treatment on the synthesis process. This treatment consists of maintaining TiO_2 particles in suspension at a temperature of 90 °C under magnetic agitation for 24 h. Our findings, based on optical, XRD, FTIR, Raman, and SEM-EDX investigations, demonstrate that this process enhances the properties of the synthesised TiO_2 NPs as exemplified by the analysis presented for sample S3. This enhancement is likely a result of the thermal treatment stage's ability to prevent or reduce the agglomeration of titanium dioxide NPs, owing to strong particles' collisions and their size reduction. This leads to a significant dispersion of TiO_2 NPs in the aqueous solution. Additionally, the process contributes to the washing of the produced tiny particles.

5. Conclusion

Using Eucalyptus plant extract as a bio-template, four distinct techniques were used to successfully synthesise TiO_2 NPs in a rapid, simple, cost-effective, and environmentally friendly approach. Three of these techniques involved the novel application of a mild thermal treatment were the TiO_2 suspension is maintained at 90 °C for 24 h under magnetic stirring. Using various characterisation techniques, the properties of the four samples were accurately determined. The FT-IR and Raman spectra revealed that all the synthesised TiO_2 NPs are primarily associated to the mainly pure tetragonal anatase phase with an O-Ti-O characteristic band around 580 cm^{-1}, whereas the SEM analysis revealed the NPs spherical shapes. The proposed thermal treatment also produces NPs with smaller sizes closely resembling those of commercial TiO_2. The presented methodology is a promising alternative to conventional TiO_2 manufacturing techniques which typically rely on harsh reaction conditions (high temperatures and/or high pressures). In contrast, the utilization of Eucalyptus plant extract, coupled with the described thermal treatment introduces a more sustainable approach. With its emphasis on simplicity and efficiency, this method represents a significant advancement in TiO_2 synthesis, opening up new avenues for application across various fields in the bioengineering, electronic, environmental, biological, and medical sectors.

CRediT authorship contribution statement

Abouelkacem Sahraoui: Writing – original draft, Methodology, Investigation, Formal analysis, Conceptualization. **Mouna Hamlaoui:** Investigation, Formal analysis. **Sara Chikhi:** Investigation, Formal analysis. **Safia Harrat:** Investigation, Formal analysis. **Oualid Baghriche:** Methodology, Conceptualization. **Abdennour Zertal:** Writing – review & editing, Writing – original draft, Validation, Supervision, Methodology, Conceptualization. **Sergio Vernuccio:** Writing – review & editing.

Declaration of competing interest

The authors declare that they have no known competing financial interests or personal relationships that could have appeared to influence the work reported in this article.

Acknowledgements

The authors express their gratitude to Constantine 1 - Frères Mentouri University for providing the sample analysis facilities required to complete the task.

Data availability

No data was used for the research described in the article.

References

[1] M. Sharma, K. Behl, S. Nigam, M. Joshi, TiO_2-GO nanocomposite for photocatalysis and environmental applications: a green synthesis approach, Vacuum 156 (2018) 434–439, https://doi.org/10.1016/j.vacuum.2018.08.009.
[2] G. Lusvardi, C. Barani, F. Giubertoni, G. Paganelli, Synthesis and characterization of TiO_2 nanoparticles for the reduction of water pollutants, Materials 10 (2017) 1208, https://doi.org/10.3390/ma10101208.
[3] H. Zhang, J.F. Banfield, Structural characteristics and mechanical and thermodynamic properties of nanocrystalline TiO_2, Chem. Rev. 114 (2014) 9613–9644.
[4] P. Magalhães, L. Andrade, O.C. Nunes, A. Mendes, Titanium dioxide photocatalysis: fundamentals and application on photoinactivation, Rev. Adv. Mater. Sci. 51 (2017) 91–129.
[5] J. Bai, B. Zhou, Titanium dioxide nanomaterials for sensor applications, Chem. Rev. 114 (2014) 10131–10176, https://doi.org/10.1021/cr400625j.
[6] Y. Ma, X.L. Wang, Y.S. Jia, X.B. Chen, H.X. Han, C. Li, Titanium dioxide-based nanomaterials for photocatalytic fuel generations, Chem. Rev. 114 (2014) 9987–10043, https://doi.org/10.1021/cr500008u.
[7] P. Kern, P. Schwaller, J. Michler, Electrolytic deposition of titania films as interference coatings on biomedical implants: microstructure, chemistry and nano-mechanical properties, Thin Solid Films 494 (2006) 279–286, https://doi.org/10.1016/j.tsf.2005.09.068.
[8] S. Hore, C. Vetter, R. Kern, H. Smit, A. Hinsch, Influence of scattering layers on efficiency of dye-sensitized solar cells, Sol. Energ. Mat. Sol. C. 90 (2006) 1176–1188, https://doi.org/10.1016/j.solmat.2005.07.002.
[9] A. Weir, P. Westerhoff, L. Fabricius, K. Hristovski, N. von Goetz, Titanium dioxide nanoparticles in food and personal care products, Environ. Sci. Technol. 46 (2012) 2242–2250, https://doi.org/10.1021/es204168d.
[10] W. Ahmad, K.K. Jaiswal, S. Soni, Green synthesis of titanium dioxide (TiO_2) nanoparticles by using Mentha arvensis leaves extract and its antimicrobial properties, Inorg. Nano-Metal. Chem. 50 (2020) 1032–1038, https://doi.org/10.1080/24701556.2020.1732419.
[11] R. Katal, S. Masudy-Panah, M. Tanhaei, M. Farahani, H. Jiangyong, Review on the synthesis of the various types of anatase TiO_2 facets and their applications for photocatalysis, Chem. Eng. J. 384 (2020) 1–78, https://doi.org/10.1016/j.cej.2019.123384.
[12] S. Sungur, Titanium dioxide nanoparticles, in: Handbook of Nanomaterials and Nanocomposites for Energy and Environmental Applications, Springer, Cham, 2021, pp. 713–730, https://doi.org/10.1007/978-3-030-11155-7.
[13] A. Chemsiddine, H. Jungblut, S. Boulmaaz, Investigation of the nanocluster self-assembly process by scanning tunneling microscopy and optical spectroscopy, J. Phys. Chem. B 100 (1996) 12546–12551, https://doi.org/10.1021/jp960229u.
[14] C.J. Barbe, F. Arendse, F. Lenzmann, M. Gratzel, P. Comte, M. Jirousek, V. Shklover, Nanocrystalline titanium oxide electrodes for photovoltaic applications, J. Am. Ceram. Soc. 80 (1997) 3157–3171, https://doi.org/10.1111/j.11512916.1997.tb03245.x.
[15] H. Mori, H. Yin, S. Kambe, S. Murasawa, Y. Wada, S. Yanagida, T. Kitamura, T. Sakata, Hydrothermal synthesis of nanosized anatase and rutile TiO_2 using amorphous phase TiO_2, J. Mater. Chem. 11 (2001) 1694–1703.
[16] A. Kornowski, H. Weller, P.D. Cozzoli, Low-temperature synthesis of soluble and processable organic-capped anatase TiO_2 nanorods, J. Am. Chem. Soc. 125 (2003) 14539–14548, https://doi.org/10.1021/ja036505h.
[17] R.A. Metwally, J. El Nady, S. Ebrahim, A. El Sikaily, N.A. El-Sersy, S.A. Sabry, H. A. Ghozlan, Biosynthesis, characterization and optimization of TiO_2 nanoparticles by novel marine halophilic *Halomonas* sp. RAM2: application of natural dye-sensitized solar cells, Microb. Cell Fact. 22 (2023) 78, https://doi.org/10.1186/s12934-023-02093-3.
[18] Z.L. Azizi, S. Daneshjou, Bacterial nano-factories as a tool for the biosynthesis of TiO_2 nanoparticles: characterization and potential application in wastewater treatmen, Appl. Biochem. Biotechnol. 196 (2024) 5656–5680, https://doi.org/10.1007/s12010-023-04839-6.
[19] M. Srinivasan, M. Venkatesan, V. Arumugam, G. Natesan, N. Saravanan, S. Murugesan, S. Ramachandran, R. Ayyasamy, A. Pugazhendhi, Green synthesis and characterization of titanium dioxide nanoparticles (TiO_2 NPs) using Sesbania grandiflora and evaluation of toxicity in zebrafish embryos, Process Biochem. 80 (2019) 197–202.
[20] T. Santhoshkumar, A.A. Rahuman, C. Jayaseelan, G. Rajakumar, S. Marimuthu, A. V. Kirthi, K. Velayutham, J. Thomas, J. Venkatesan, S.K. Kim, Green synthesis of titanium dioxide nanoparticles using Psidium guajava extract and its antibacterial and antioxidant properties, Asian Pac. J. Trop. Med. (2014) 968–976, https://doi.org/10.1016/S1995-7645(14)60171-1.
[21] J. Rajkumari, C.M. Magdalane, B. Siddhardha, J. Madhavan, G. Ramalingam, N. A. Al-Dhabi, M.V. Arasu, A. Ghilan, V. Duraipandiayan, K. Kaviyarasu, Synthesis of titanium oxide nanoparticles using Aloe barbadensis mill and evaluation of its antibiofilm potential against Pseudomonas aeruginosa PAO1, J. Photochem. Photobiol., B 201 (2019) 111667, https://doi.org/10.1016/j.jphotobiol.2019.111667.
[22] A. Ansari, V. Siddiqui, W. Ui Rehman, A.M. Khursheed, W. Siddiqi, A. Alosaimi, M. Hussein, M. Rafatullah, Green synthesis of TiO_2 nanoparticles using Acorus calamus leaf extract and evaluation its photocatalytic and in vitro antimicrobial activity, Catalysts 12 (2022) 181, https://doi.org/10.3390/catal9100799.
[23] G. Nabi, W. Raza, M.B. Tahir, Green synthesis of TiO_2 nanoparticle using cinnamon powder extract and the study of optical properties, J. Inorg Organomet P. 30 (2019) 1425–1429. https://link.springer.com/article/10.1007/s10904-019-01248-3.
[24] D. Rueda, V. Arias, Y. Zhang, A. Cabot, A.C. Agudelo, D. Cadavid, Low-cost tangerine peel waste mediated production of titanium dioxide nanocrystals: synthesis and characterization, Environ. Nanotechnol. Monit. Manag. 13 (2020) 100285, https://doi.org/10.1016/j.enmm.2020.100285.
[25] S. Ponarulselvam, C. Panneerselvam, K. Murugan, N. Aarthi, K. Kalimuthu, S. Thangamani, Synthesis of silver nanoparticles using leaves of Catharanthus roseus linn. G. Don and their ant plasmodial activities, Asian Pac. J. Trop. Biomed. 2 (2012) 574–580, https://doi.org/10.1016/S2221-1691(12)60100-2.

[26] P. Rajasekharreddy, P.U. Rani, Biofabrication of Ag nanoparticles using Sterculia foetida L. seed extract and their toxic potential against mosquito vectors and HeLa cancer cells, Mater. Sci. Eng. C. 39 (2014) 203–212, https://doi.org/10.1016/j.msec.2014.03.003.

[27] A. Verma, M.S. Mehata, Controllable synthesis of silver nanoparticles using neem leaves and their antimicrobial activity, J. Radiat. Res. Appl. Sci. 9 (2016) 109–115, https://doi.org/10.1016/j.jrras.2015.11.001.

[28] M.A. Irshad, R. Nawaz, M. Zia urRehman, M. Imran, M.J. Ahmad, S. Ahmad, A. Inaam, A. Razzaq, M. Rizwan, S. Ali, Synthesis and characterization of titanium dioxide nanoparticles by chemical and green methods and their antifungal activities against wheat rust, Chemosphere 258 (2020) 127352, https://doi.org/10.1016/j.chemosphere.2020.127352.

[29] X. Zhu, K. Pathakoti, H.M. Hwang, Chapter 10. Green Synthesis of Titanium Dioxide and Zinc Oxide Nanoparticles and their Usage for Antimicrobial Applications and Environmental Remediation. Green Synthesis, Characterization and Applications of Nanoparticles, Elsevier Inc., 2019, pp. 223–263, https://doi.org/10.1016/B978-0-08-1025796.00010-1.

[30] A.A. Barzinjy, H.H. Azeez, Green synthesis and characterization of zinc oxide nanoparticles using Eucalyptus globulus labill leaf extract and zinc nitrate hexahydrate salt, SN Appl. Sci. 2 (2020) 991, https://doi.org/10.1007/s42452-020-2813-1.

[31] M. Aravind, M. Amalanathan, M. Sony Michael Mary, Synthesis of TiO_2 nanoparticles by chemical and green synthesis methods and their multifaceted properties, SN Appl. Sci. 3 (2021) 409, https://doi.org/10.1007/s42452-021-04281-5.

[32] M.I.H. Brooker, A.V. Slee, Eucalyptus, in: N.G. Walsh, T.J. Entwisle (Eds.), Flora of Victoria Vol. 3, Dicotyledons Winteraceae to Myrtaceae, Inkata Press, Melbourne, 1996, pp. 946–1009.

[33] Z.C. Zhuang, L.L. Huang, F.F. Wang, Z.L. Chen, Effects of cyclodextrin on the morphology and reactivity of iron-based nanoparticles using eucalyptus leaf extract, Ind. Crop. Prod. 69 (2015) 308–313, https://doi.org/10.1016/j.indcrop.2015.02.027.

[34] T. Wang, X.Y. Jin, Z.L. Chen, M. Megharaj, R. Naidu, Green synthesis of Fe nanoparticles using eucalyptus leaf extracts for treatment of eutrophic wastewater, Sci. Total Environ. 466–467 (2014) 210–213, https://doi.org/10.1016/j.scitotenv.2013.07.022.

[35] V. Madhavi, T.N.V.K.V. Prasad, A.V.B. Reddy, B.R. Reddy, G. Madhavi, Application of phytogenic zerovalent iron nanoparticles in the adsorption of hexavalent chromium, Spectrochim. Acta 116 (2013) 17–25, https://doi.org/10.1016/j.scitotenv.2013.07.022.

[36] X. Weng, M. Guo, F. Luo, Z. Chen, One-step green synthesis of bimetallic Fe/Ni nanoparticles by eucalyptus leaf extract: biomolecules identification, characterization and catalytic activity, Chem. Eng. J. 308 (2017) 904–911, https://doi.org/10.1016/j.cej.2016.09.134.

[37] Y. Mo, Y. Tang, S. Wang, J. Ling, H. Zhang, D. Luo, Green synthesis of silver nanoparticles using eucalyptus leaf extract, Mater. Lett. 144 (2015) 165–167, https://doi.org/10.1016/j.matlet.2015.01.004.

[38] X. Jin, N. Li, X. Weng, C. Li, Z. Chen, Green reduction of graphene oxide using *eucalyptus* leaf extract and its application to remove dye, Chemosphere 208 (2018) 417–424, https://doi.org/10.1016/j.chemosphere.2018.05.199.

[39] G. Ghoshal, D. Singh, Synthesis and characterization of starch nanocellulosic films incorporated with Eucalyptus globulus leaf extract, Int. J. Food Microbiol. 332 (2020) 108765, https://doi.org/10.1016/j.ijfoodmicro.2020.108765.

[40] D.J. Bhuyan, Q.V. Vuong, A.C. Chalmers, I.A. van Altena, M.C. Bowyer, C. J. Scarlett, Phytochemical, antibacterial and antifungal properties of an aqueous extract of eucalyptus microcorys leaves, S. Afr. J. Bot. 112 (2017) 180–185, https://doi.org/10.1016/j.sajb.2017.05.030.

[41] F. Al Qarni, N.A. Alomair, H.H. Mohamed, Environment - friendly nanoporous titanium dioxide with enhanced photocatalytic activity, Catalysts 9 (2019) 799, https://doi.org/10.3390/catal9100799.

[42] C. Li, Z. Zhuang, X. Jin, Z. Chen, A facile and green preparation of reduced graphene oxide using eucalyptus leaf extract, Appl. Surf. Sci. 422 (2017) 469–474, https://doi.org/10.1016/j.apsusc.2017.06.032.

[43] K. Wang, Y. Liu, X. Jin, Z. Chen, Characterization of iron nanoparticles/reduced graphene oxide composites synthesized by one step eucalyptus leaf extract, Environ. Pollut. 250 (2019) 8–13, https://doi.org/10.1016/j.apsusc.2017.06.032.

[44] B. Ajitha, Y. Ashok Kumar Reddy, P.S. Reddy, Biogenic nano-scale silver particles by Tephrosia purpurea leaf extract and their inborn antimicrobial activity, Spectrochim. Acta 121 (2014) 164–172, https://doi.org/10.1016/j.saa.2013.10.077.

[45] K.M. Reddy, S.V. Manorama, A.R. Reddy, Bandgap studies on anatase titanium dioxide nanoparticles, Mater. Chem. Phys. 78 (2002) 239–245, https://doi.org/10.1016/S0254-0584(02)00343-7.

[46] A. Jayachandran, T.R. Aswathy, A.S. Nair, Green synthesis and characterization of zinc oxide nanoparticles using Cayratia pedata leaf extract, Biochem. Biophys. Reports 26 (2021) 100995, https://doi.org/10.1016/j.bbrep.2021.100995.

[47] M. Noruzia, D. Zare, K. Khoshnevisan, D. Davoodi, Rapid green synthesis of gold nanoparticles using Rosa hybrida petal extract at room temperature, Spectrochim. Acta 79 (2011) 1461–1465, https://doi.org/10.1016/j.saa.2011.05.001.

[48] H. Abdul Salam, R. Sivaraj, Ocimum basilicum L. Var. purpurascens Benth.-LAMIACEAE mediated green synthesis and characterization of titanium dioxide nanoparticles, Adv. Bio. Res. 5 (2014) 10–16, https://doi.org/10.15515/abr.0976-4585.5.3.1016.

[49] S. Bagheri, K. Shameli, S.B. Abd Hamid, Synthesis and characterization of anatase titanium dioxide nanoparticles using egg white solution via sol-gel method, J. Chem. (2013) 848205, https://doi.org/10.1155/2013/848205.

[50] H.H. Mohamed, Biphasic TiO_2 microspheres/reduced graphene oxide for effective simultaneous photocatalytic reduction and oxidation processes, Appl. Catal. A-Gen. 541 (2017) 25–34, https://doi.org/10.1016/j.apcata.2017.04.017.

[51] S. Subhapriya, P. Gomathipriya, Green synthesis of titanium dioxide (TiO_2) nanoparticles by Trigonella foenum-graecum extract and its antimicrobial properties, Microb. Pathogenesis 116 (2018) 215–220, https://doi.org/10.1016/j.micpath.2018.01.027.

[52] S. Kaviya, E. Prasad, Eco-friendly synthesis of ZnO nano pencils in aqueous medium: a study of photocatalytic degradation of methylene blue under direct sunlight, RSC Adv. 6 (2016) 33821–33827, https://doi.org/10.1039/C6RA04306B.

[53] R.A. Solano, A.P. Herrera, D. Maestre, A. Cremades, Fe-TiO_2 nanoparticles synthesized by green chemistry for potential application in waste water photocatalytic treatment, J. Nanotechnol. (2019) 2–13, https://doi.org/10.1155/2019/4571848.

[54] T. Ali, P. Tripathi, A. Azam, W. Raza, A. S Ahmed, A. Ahmed, M. Muneer, Photocatalytic performance of Fe-doped TiO_2 nanoparticles under visible-light irradiation, Mater. Res. Express 4 (2017) 015022, https://doi.org/10.1088/2053-1591/aa576d.

[55] M.B. Muneer, H.K. Abdul Amir, B.M. Abu, S.K. Mohd, S. Kamaruzzaman, Synthesis and catalytic activity of TiO_2 nanoparticles for photochemical oxidation of concentrated chlorophenols under direct solar radiation, Int. J. Electrochem. Sci. 7 (2012) 4871–4888, https://doi.org/10.1016/S1452-3981(23)19588-5.

[56] J. Singh, T. Dutta, K.H. Kim, M. Rawat, P. Samddar, P. Kumar, Green synthesis of metals and their oxide nanoparticles: applications for environmental remediation, J. Nanobiotechnol. 16 (2018) 1–24, https://doi.org/10.1186/s12951-018-0408-4.